

Efficiency Optimization and Component Selection for Propulsion Systems of Electric Multicopters

Xunhua Dai , Quan Quan , Jinrui Ren , and Kai-Yuan Cai

Abstract—Currently, the time of endurance of electric multicopters is still too short for many mission requirements, and optimizing the efficiency of the propulsion system is considered as an effective way to overcome this problem. This paper proposes a practical method to help designers quickly select the optimal products of the propulsion system to maximize the multicopter efficiency under the desired flight condition. First, the modeling methods for the components of the propulsion system are studied respectively to describe the optimization problem mathematically. Second, methods are proposed to find optimal motor and propeller combination with the maximum thrust efficiency according to the given design requirements. Finally, factors that may affect the hovering time of multicopters are analyzed, and the optimal battery parameters are obtained for maximizing the multicopter endurance. Experiments and simulations are performed to demonstrate the effectiveness and practicability of the proposed method.

Index Terms—Efficiency, multicopter, optimization design, propulsion system, unmanned aerial vehicles (UAVs).

I. INTRODUCTION

DURING recent years, multicopter unmanned aerial vehicles (UAVs) are becoming increasingly important in both civil and military fields [1], [2]. However, the time of endurance of electric multicopters is still too short for many mission requirements, which is an important factor hindering the further development of the multicopter field. Limited by the battery technology, optimizing the efficiency of the propulsion system is a practical and effective way to improve the endurance of multicopters.

According to [3], a typical propulsion system usually consists of a battery pack and several propulsion units [including

a propeller, a brushless direct-current (BLDC) motor, and an electronic speed control (ESC)]. Among these components, the motor and the propeller are the most important components to determine the efficiency of a propulsion system [4], [5]. However, the efficiency of a motor-propeller system is not a constant value but a variable value that depends on the motor parameters, the propeller parameters, and the actual flight condition. For example, an efficient propeller and an efficient motor may result in an inefficient propulsion system, because the propeller makes the motor work under its inefficient state. Since there are thousands of motor and propeller products on the market, a large number of try-and-error experiments are usually required to determine an efficient motor and propeller combination to satisfy the desired design requirements. Thus, a method to help designers quickly determine the optimal propulsion system will be beneficial to reduce development time and cost [6].

There are studies on the efficiency analysis [7] and design optimization [8], [9] of propellers. However, according to [3], the motor and propeller should be treated as a whole because their efficiencies are coupled with each other. Some design experiences are introduced in [3], such as a motor with a low KV value (motor velocity constant) should match with a propeller with a large diameter for higher whole efficiency. However, these experiences are concluded from experiments, so one objective of this paper is to use theoretical analysis to explain and verify these design experiences. Since separately optimizing the motor or the propeller cannot give the desired result, optimization methods for the whole propulsion systems of fixed-wing aircraft [10]–[12] and multicopters [13], [14] are studied in recent years. Most of them adopt numerical methods to search and traverse all the possible propulsion component combinations in the prepared motor and propeller database based on the proposed cost functions. However, these numerical methods are time consuming and require a large motor and propeller product database to obtain a practical result. Besides, the numerical search methods can only find the local optimal solution within the database scope, which is unable to discover the better multicopter designs that have not been included in the database.

In our previous research [15], based on the mathematical modeling methods, a practical and analytic method is proposed to estimate the flight performance of a multicopter with known component parameters of the propulsion system. The study in this paper is an extension of our previous work presented in [15], namely finding the optimal propulsion system components

Manuscript received May 23, 2018; revised August 14, 2018 and September 29, 2018; accepted November 26, 2018. Date of publication December 19, 2018; date of current version May 31, 2019. This work was supported by the National Key Project of Research and Development Plan under Grant 2016YFC1402500. (Corresponding author: Quan Quan.)

X. Dai, J. Ren, and K.-Y. Cai are with the School of Automation Science and Electrical Engineering, Beihang University, Beijing 100191, China (e-mail: dai@buaa.edu.cn; renjinrui@buaa.edu.cn; kycai@buaa.edu.cn).

Q. Quan is with the School of Automation Science and Electrical Engineering, Beihang University, Beijing 100191, China, and also with the State Key Laboratory of Virtual Reality Technology and Systems, Beihang University, Beijing 100191, China (e-mail: qq_buaa@buaa.edu.cn).

Color versions of one or more of the figures in this paper are available online at <http://ieeexplore.ieee.org>.

Digital Object Identifier 10.1109/TIE.2018.2885715

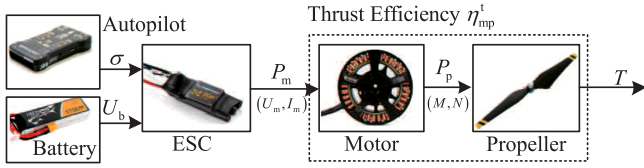


Fig. 1. Power transmission diagram of multicopter propulsion systems.

according to the given design requirements. This paper proposes an analytic method to estimate the optimal propeller parameters based on the modeling methods presented in [15]. Then, the motor and its optimal matching propeller are treated as a combination to find the optimal motor–propeller combination that satisfies the design requirements of the propulsion system. Finally, factors that may affect the hovering time of multicopters are analyzed, and the optimal battery parameters are obtained for maximizing the multicopter endurance.

The main contributions of this paper are as follows.

- 1) Compared with the current studies, this paper uses analytical methods to analyze the efficiency optimization problem, and derives the expressions to obtain the globally optimal solution.
- 2) The proposed method can quickly obtain the global optimal solution for the multicopter design, which is beneficial for improving the design and verification speed of multicopters and reducing the cost of development and experimental verification.
- 3) The conclusions derived from the theoretical analysis have great guiding significance for designers to improve the time of endurance of multicopters, which may broaden the application scopes of multicopter UAVs.

The paper is organized as follows. Section II gives a comprehensive analysis of the design optimization task to transform it into a mathematical optimization problem. Then, based on the mathematical models of the motor and the propeller, the optimization methods for the propeller and the motor are presented in Section III. In Section IV, experiments are performed to demonstrate the effectiveness and practicability of the proposed method. In the end, Section V presents the conclusions.

II. PROBLEM FORMULATION

A. Design Requirements

The power transmission diagram of propulsion systems is presented in Fig. 1, where the propeller output thrust T (unit: N) is controlled by the autopilot with the throttle signal $\sigma \in [0, 1]$. As throttle signal σ changes from 0 to 1, the thrust T of a single propeller changes from 0 to T_{\max} . Therefore, T_{\max} (unit: N) is called the full-throttle thrust (when $\sigma = 1$) which determines the maneuverability of a multicopter. Meanwhile, the time of endurance of a multicopter is usually defined under the hovering mode when the multicopter stays fixed in the air and relatively static to the ground. The propeller thrust under the hovering mode is called the hovering thrust T_{hover} (unit: N).

The design requirements for a multicopter propulsion system are usually given by the following parameters:

TABLE I
DEFINITIONS OF MAIN PARAMETERS IN THIS PAPER

| | |
|--------------------------------|---|
| Propeller set | $\Theta_p \triangleq \{\text{Diameter } D_p \text{ (m), Pitch Angle } \varphi_p \text{ (rad), Blade Number } B_p\}$ |
| Motor set | $\Theta_m \triangleq \{\text{Nominal Maximum Voltage } U_{m\text{Max}} \text{ (V), Nominal Maximum Current } I_{m\text{Max}} \text{ (A), KV Value } K_V \text{ (RPM/V), No-load Current } I_{m0} \text{ (A), No-load Voltage } U_{m0} \text{ (V), Resistance } R_m \text{ (\Omega)}\}$ |
| Battery & ESC set | $\Theta_b \triangleq \{\text{Nominal Voltage } U_b \text{ (unit: V), Capacity } C_b \text{ (mAh), Battery Efficiency } \eta_b, \text{ ESC Efficiency } \eta_e, \text{ Power Density } \rho_b \text{ (W}\cdot\text{h/kg)}\}$ |
| Other parameters and variables | Thrust Efficiency η_{mp}^t , Hovering Thrust T_{hover} , Air Density ρ , Full-throttle Thrust T_{\max} , Motor Constant K_E , Propeller Pitch H_p , Propeller Thrust T , Propeller Torque M , Rotating Speed N , Thrust Coefficient C_T , Torque Coefficient C_M , Blade Params $A, \varepsilon, \lambda, \zeta, e, C_{fd}$ |

- 1) the flight air density ρ (unit: kg/m^3) or the altitude h (unit: m) and the local temperature t_C (unit: $^\circ\text{C}$);
- 2) the desired hovering thrust T_{hover} ;
- 3) the desired full-throttle thrust T_{\max} .

Then, the design objective is described as finding the optimal motor and propeller combination under the desired altitude h (or air density ρ), so that: 1) the propulsion system has the maximum efficiency under the hovering mode when the propeller thrust equals to T_{hover} ; and 2) the propeller thrust has the maximum thrust T_{\max} under the full-throttle mode when the throttle signal $\sigma = 1$.

In practice, the air density ρ can be estimated from the altitude h and the local temperature t_C according to the International Standard Atmosphere model [16]. The thrust requirements T_{hover} and T_{\max} come from the top-level requirements of the multicopter design. Since the hovering thrust T_{hover} is applied to support the multicopter weight, the hovering thrust T_{hover} can be obtained with the mass m_{copter} (unit: kg) and the propeller number n_p as

$$T_{\text{hover}} = \frac{m_{\text{copter}} \cdot g}{n_p} \quad (1)$$

where $g \approx 9.8 \text{ m/s}^2$ is the acceleration of gravity. Meanwhile, the full-throttle thrust T_{\max} is determined by the maximum acceleration requirement a_c (unit: m/s^2) of the multicopter, which is defined as

$$a_c = \frac{n_p \cdot T_{\max} - m_{\text{copter}} \cdot g}{m_{\text{copter}}} \quad (2)$$

Therefore, the full-throttle thrust T_{\max} can be obtained from (2) as

$$T_{\max} = \frac{m_{\text{copter}} (g + a_c)}{n_p} \quad (3)$$

B. Component Parameters

The main parameters in this paper are listed in Table I, where $\Theta_p, \Theta_m, \Theta_b$ represent the parameter sets for propellers, motors, and batteries. In order to ensure commonality of the method, all the component parameters in $\Theta_p, \Theta_m, \Theta_b$ are the basic parameters that can be easily found in the product description pages. In this paper, the subscript ‘‘Opt’’ denotes the optimal solution

of the value, the subscript “Max” denotes the maximum value, and the subscript “Hover” denotes the value under the hovering mode.

The pitch angle φ_p (unit: rad) in Table I is defined according to the propeller diameter D_p (unit: m) and the propeller pitch H_p (unit: m) as

$$\varphi_p \triangleq \arctan \frac{H_p}{\pi D_p} \quad (4)$$

where the parameters H_p and D_p are usually contained in the propeller model name. For example, the propeller “APC 10 \times 4.7” denotes that the propeller diameter is $D_p = 10$ in = 0.254 m, and the pitch is $H_p = 4.7$ in \approx 0.11 m, which yields the pitch angle from (4) as $\varphi_p = 0.1485$ rad.

Remark 1: The parameters on the product description pages may be inaccurate, which will affect the accuracy of the optimization results. Therefore, calibrations should be made for the parameters of the motor and the propeller according to the experimental results.

C. Optimization Problem

The objective of the multicopter efficiency optimization problem is to maximize the hovering time of a multicopter, which is equivalent to minimizing the power consumption of the propulsion system for generating the same thrust. According to [3, p. 42], a widely used index called thrust efficiency η_{mp}^t (unit: N/W) is introduced here as

$$\eta_{\text{mp}}^t \triangleq \frac{T_{\text{hover}}}{P_{m\text{Hover}}} = f_{\eta_{\text{mp}}^t}(\rho, T_{\text{hover}}, \Theta_m, \Theta_p) \quad (5)$$

where ρ (unit: kg/m³) is the air density determined by the flight condition including the altitude and temperature. The thrust efficiency η_{mp}^t is not a constant value, and it has a complex nonlinear relationship $f_{\eta_{\text{mp}}^t}(\cdot)$ with the parameters $\{\Theta_m, \Theta_p\}$ and the flight condition $\{\rho, T_{\text{hover}}\}$. Noteworthy, unlike common efficiency definition, the thrust efficiency η_{mp}^t is a parameter with a unit “N/W,” which makes the optimization problem more complicated.

In summary, the optimization objective of this paper is to find the optimal motor and propeller components $\{\Theta_m, \Theta_p\}$ to maximize the thrust efficiency η_{mp}^t under the given flight condition $\{\rho, T_{\text{hover}}\}$, and then design the optimal battery for the longest time of endurance.

The optimization constraints mainly come from two aspects: the design requirement constraint and the safety constraint. The design requirement constraint is about the desired propeller full-throttle thrust T_{max} of the propulsion system. According to [15], the theoretical maximum thrust $T_{p\text{Max}}$ (unit: N) of the motor–propeller system can be estimated by parameters ρ, Θ_m, Θ_p as

$$T_{p\text{Max}} = f_{T_{p\text{Max}}}(\rho, \Theta_m, \Theta_p). \quad (6)$$

According to the statistical analysis in [17], the size and weight of a motor–propeller system are all directly related to $T_{p\text{Max}}$. Therefore, the maximum thrust $T_{p\text{Max}}$ should be chosen as close to its desired value T_{max} as possible (small error is tolerable in practice) to ensure the motor–propeller system being fully

utilized, which is described by

$$\left| \frac{T_{p\text{Max}} - T_{\text{max}}}{T_{\text{max}}} \right| \leq \varepsilon_T \quad (7)$$

where ε_T is a small positive threshold coefficient.

The safety constraint of a propulsion system in this paper denotes that the voltage and current of a motor should work within the allowance ranges to prevent the motor from being overheated. The motor voltage and current are constrained by parameters $U_{m\text{Max}}$ and $I_{m\text{Max}}$ in Table I as

$$U_m \leq U_{m\text{Max}}, I_m \leq I_{m\text{Max}} \quad (8)$$

where U_m and I_m are the equivalent direct-current voltage and current of a BLDC motor [15].

D. Solving Procedures

The above optimization problem is very difficult to solve through conventional methods, because

- 1) the parameters in Θ_m and Θ_p are both stored in the database in discrete forms;
- 2) the mathematical expressions of $f_{\eta_{\text{mp}}^t}(\cdot)$ and $f_{T_{p\text{Max}}}(\cdot)$ are highly nonlinear and very complex;
- 3) it is hard to solve more than eight variables in Θ_m, Θ_p through only three constraints in (7) and (8).

Therefore, most of the existing studies adopt numerical methods to search and traverse all the possible motor and propeller combinations to find the optimal one.

In order to solve this optimization problem, an analytic method is proposed to obtain the optimal propeller for a given motor, and then a numerical method is used to find the optimal motor product from the database. For convenience, the optimal motor, propeller, and battery obtained from the optimization problem are represented by $\Theta_{p\text{Opt}}, \Theta_{m\text{Opt}},$ and $\Theta_{b\text{Opt}}$. The key solving procedures are presented below.

- 1) *Mathematical Modeling:* Obtain the expressions of $f_{\eta_{\text{mp}}^t}(\cdot)$ and $f_{T_{p\text{Max}}}(\cdot)$ according to the mathematical models of the propeller and the motor.
- 2) *Propeller Optimization:* Obtain the optimal propeller $\Theta_{p\text{Opt}}$ for any given motor Θ_m , so that the motor and the propeller combination has the maximum thrust efficiency η_{mp}^t .
- 3) *Motor Optimization:* Find the optimal motor–propeller combination $\{\Theta_{m\text{Opt}}, \Theta_{p\text{Opt}}\}$ that satisfies the constraints in (7) and (8) and has the maximum thrust efficiency η_{mp}^t .
- 4) *Battery Optimization:* Design the optimal battery $\Theta_{b\text{Opt}}$ for the longest hovering time.

III. DESIGN OPTIMIZATION

This section successively introduces the detailed four solving procedures as mentioned in the previous section.

A. Mathematical Modeling

The electric motors used in multicopters are BLDC motors. According to the modeling method in [15], a BLDC motor is a synchronous three-phase permanent magnet motor, which can be modeled as a permanent magnet direct-current motor with the

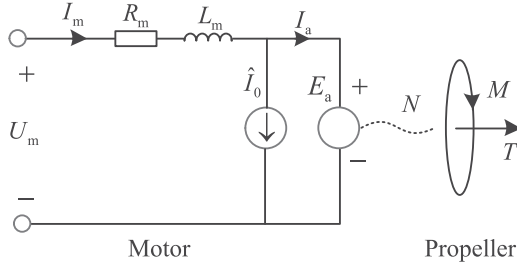


Fig. 2. Equivalent circuit model of the motor-propeller system.

equivalent circuit shown in Fig. 2. For a multicopter, fixed-pitch propellers are often used, and there are many methods to model the aerodynamic characteristics of fixed-pitch propellers [18], [19]. Then, the mathematical expression of the thrust efficiency η_{mp}^t can be obtained based on the motor and propeller models, which will be further used to derive the optimization solution of the component selection.

1) Propeller Modeling: According to [18], the thrust force T (unit: N) and torque M (unit: N·m) of the fixed-pitch propeller can be obtained through following equations:

$$\begin{cases} T = C_T \cdot \rho \cdot \left(\frac{N}{60}\right)^2 \cdot D_p^4 \\ M = C_M \cdot \rho \cdot \left(\frac{N}{60}\right)^2 \cdot D_p^5 \end{cases} \quad (9)$$

where N (unit: r/min) is the propeller rotating speed, ρ is the local air density (unit: kg/m³), C_T is the propeller thrust coefficient, C_M is the propeller torque coefficient, and D_p is the propeller diameter.

The propeller coefficients C_T and C_M of multicopters under hovering mode are modeled by the blade element theory by combining results in [15], [19] as

$$\begin{cases} C_T = \frac{0.27\pi^3 \lambda \zeta^2 K_0 \varepsilon}{\pi A + K_0} B_p^{\alpha_t} \varphi_p \\ C_M = \frac{1}{4A} \pi^2 \lambda \zeta^2 B_p \left(C_{fd} + \frac{\pi A K_0^2 \varepsilon^2}{e(\pi A + K_0)^2} \varphi_p^2 \right) \end{cases} \quad (10)$$

where $A, \varepsilon, \lambda, \zeta, e, C_{fd}$ are blade parameters determined by the airfoil shape of a propeller blade [15], $\alpha_t \approx 0.85 - 0.9$ is a correction parameter for C_T affected by the blade interference [19], and D_p, φ_p, B_p are propeller parameters determined by the extension, distortion, and combination of the propeller blades. The blade parameter optimization for $A, \varepsilon, \lambda, \zeta, e, C_{fd}, \alpha_t$ has been well studied in [20]–[22], and there are many efficient blade airfoils adopted by propeller manufacturers, like Clark Y. Since the blade shapes for a certain series of propellers are the same, the blade parameters $A, \varepsilon, \lambda, \zeta, e, C_{fd}$ can be treated as constant values, and this paper focuses on obtaining the optimal propeller parameters D_p, φ_p, B_p for a multicopter.

2) Motor Modeling: A BLDC motor is driven by the three-phase PWM-modulated voltage control signal from ESC [3], [23], which is difficult to measure and analyze because the voltage and current of the motor are not direct-current values. Therefore, a common direct-current equivalent circuit [15] as presented in Fig. 2 is useful for BLDC motor analysis. The steady-state voltage and current on the equivalent circuit are called the motor equivalent voltage U_m (unit: V) and equivalent

current I_m (unit: A). According to [15], U_m and I_m are obtained through

$$\begin{cases} I_m = \frac{\pi}{30K_E} M + I_{m0} \\ U_m = I_m R_m + K_E N \end{cases} \quad (11)$$

where K_E is the motor constant defined as

$$K_E \triangleq \frac{U_{m0} - I_{m0} R_m}{K_V U_{m0}} \quad (12)$$

in which I_{m0}, K_V, R_m, U_{m0} are the motor parameters in Table I, and M and N are the propeller torque and rotating speed from the propeller model in (9). Note that the nominal motor resistance R_{m0} on the product description is usually not accurate enough, so a resistance identification expression is derived from (11) as $R_m \approx (U_b - N^*/K_V)/I_m^* \approx 2.5R_{m0}$, where I_m^* and N^* are motor current and rotating speed in full-throttle mode.

3) Battery Modeling: As shown in Fig. 1, the motor power P_m is converted by the ESC and supplied by the battery. The battery output power P_b can be estimated by

$$P_b = n_p \cdot \frac{P_m}{\eta_e \eta_b} \quad (13)$$

where η_e is the conversion efficiency of ESC and η_b is the battery efficiency which is related to resistance, temperature and aging degree. The battery power density ρ_b (unit: W·h/kg) is defined as

$$\rho_b = \frac{P_b \cdot t_{\text{hover}}}{60 \cdot m_{\text{battery}}} = \frac{C_b U_b}{1000 \cdot m_{\text{battery}}} \quad (14)$$

where t_{hover} (unit: min) is the hovering time (battery discharge time) of the multicopter, m_{battery} (unit: kg) is the battery weight, and C_b, U_b are the battery capacity and voltage.

4) Thrust Efficiency: Substituting $T = T_{\text{hover}}$ into (9) gives

$$\begin{cases} N_{\text{hover}} = \frac{60}{D_p^2} \sqrt{\frac{T_{\text{hover}}}{\rho C_T}} \\ M_{\text{hover}} = \frac{C_M D_p}{C_T} T_{\text{hover}} \end{cases} \quad (15)$$

where N_{hover} (unit: r/min) and M_{hover} (unit: N·m) are the propeller speed and torque under the hovering mode. Unlike other motor systems, according to (9), the motor load of a multicopter (related to propeller torque M) is in quadratic growth with the propeller rotating speed N . Therefore, the motor current under the hovering mode I_m is far larger than the no-load current I_{m0} , namely $I_{m0} \ll I_m$. As a result, it is reasonable to simplify the motor model by letting $I_{m0} \approx 0$ in (11). By combining (11)–(15), the motor voltage $U_{m\text{Hover}}$ and current $I_{m\text{Hover}}$ under the hovering mode are obtained and simplified as

$$\begin{cases} I_{m\text{Hover}} = \frac{\pi C_M D_p}{30 K_E C_T} T_{\text{hover}} \\ U_{m\text{Hover}} = \frac{\pi C_M D_p}{30 K_E C_T} T_{\text{hover}} R_m + \frac{60 K_E}{D_p^2} \sqrt{\frac{T_{\text{hover}}}{\rho C_T}} \end{cases} \quad (16)$$

Meanwhile, according to [15], the motor input power $P_{m\text{Hover}}$ under the hovering mode is obtained as

$$P_{m\text{Hover}} = U_{m\text{Hover}} \cdot I_{m\text{Hover}} \quad (17)$$

Thus, by combining (10), (16), (17), the total thrust efficiency of the motor-propeller system η_{mp}^t is obtained as

$$\begin{aligned}\eta_{mp}^t &\triangleq \frac{T_{\text{hover}}}{P_{m\text{Hover}}} = \frac{T_{\text{hover}}}{U_{m\text{Hover}} \cdot I_{m\text{Hover}}} \\ &= \frac{1}{\left(\frac{\pi C_M D_p}{30 K_E C_T}\right)^2 R_m T_{\text{hover}} + \frac{2\pi C_M}{D_p \sqrt{\rho C_T^3}} \sqrt{T_{\text{hover}}}} \\ &= f_{\eta_{mp}^t}(\rho, T_{\text{hover}}, \Theta_m, \Theta_p).\end{aligned}\quad (18)$$

Some obvious conclusions can be obtained from (18) that η_{mp}^t has negative relationships with T_{hover} and R_m and η_{mp}^t has positive relationships with ρ and K_E . Moreover, if I_{m0} is considered in (16), it is easy to conclude that η_{mp}^t also has a negative relationship with I_{m0} . The above conclusions are practical for the design and efficiency analysis of multicopters.

5) Maximum Propeller Thrust and Diameter: In order to prevent the motor from being overheated and burnout, the following constraints should be satisfied:

$$U_m \leq U_{m\text{Max}}, I_m \leq I_{m\text{Max}} \quad (19)$$

where $U_{m\text{Max}}$ and $I_{m\text{Max}}$ are motor parameters from Θ_m . By substituting the maximum values $U_m = U_{m\text{Max}}$ and $I_m = I_{m\text{Max}}$ into (11), the maximum torque M_{max} (unit: N·m) and the maximum rotating speed N_{max} (unit: r/min) are obtained as

$$\begin{cases} N_{\text{max}} = \frac{(U_{m\text{Max}} - R_m I_{m\text{Max}})}{K_E} \\ M_{\text{max}} = \frac{30(I_{m\text{Max}} - I_{m0})K_E}{\pi} \end{cases} \quad (20)$$

Then, substituting $M = M_{\text{max}}$ and $N = N_{\text{max}}$ into (9), the propeller has the maximum theoretical thrust $T_{p\text{Max}}$ obtained as

$$T_{p\text{Max}} = \sqrt[5]{\frac{255(I_{m\text{Max}} - I_{m0})^4 (U_{m\text{Max}} - R_m I_{m\text{Max}})^2 \rho C_T^5 K_E^2}{\pi^4 C_M^4}} \quad (21)$$

and the propeller diameter $D_{p\text{Max}}$ is obtained as

$$D_{p\text{Max}} = \sqrt[5]{\frac{108\,000(I_{m\text{Max}} - I_{m0})K_E^3}{\pi(U_{m\text{Max}} - R_m I_{m\text{Max}})^2 \rho C_M}} \quad (22)$$

B. Propeller Optimization

1) Optimal Blade Number: By substituting (10) into (18), the thrust efficiency η_{mp}^t is written as

$$\eta_{mp}^t = \frac{1}{k_{b1} B_p^{2(1-\alpha_t)} + k_{b2} B_p^{(1-1.5\alpha_t)}} \quad (23)$$

where k_{b1} , k_{b2} are positive values irrelevant to B_p . It can be verified from (23) that η_{mp}^t monotonously decreases as B_p increases in most actual design situations ($B_p \leq 5$). As a result, the blade number B_p should be chosen as small as possible to maximize the thrust efficiency η_{mp}^t . However, in practice, the number of blades should satisfy the constraint $B_p \geq 2$ for symmetrical distribution requirement to ensure propeller dynamic balance [3, pp. 29–30]. Thus, the optimal blade number $B_{p\text{Opt}}$ should be chosen as

$$B_{p\text{Opt}} = 2. \quad (24)$$

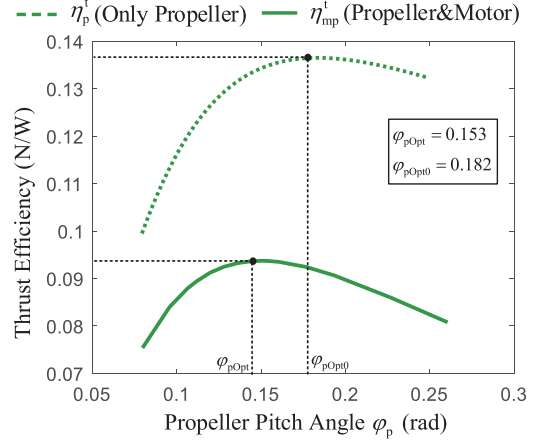


Fig. 3. Relationship between thrust efficiency and propeller pitch angle.

2) Optimal Pitch Angle: By substituting the expressions of C_T and C_M from (10) into (18), the thrust efficiency η_{mp}^t is written as

$$\eta_{mp}^t = \frac{\varphi_p^2}{k_{\varphi 1} + k_{\varphi 2} \varphi_p^{0.5} + k_{\varphi 3} \varphi_p^2 + k_{\varphi 4} \varphi_p^{2.5} + k_{\varphi 5} \varphi_p^4} \quad (25)$$

where $k_{\varphi 1} \sim k_{\varphi 5}$ are positive values irrelevant to φ_p . According to the curve analysis for (25), the thrust efficiency η_{mp}^t first increases then decreases as φ_p increases from 0 to ∞ . Therefore, there is an optimal solution $\varphi_{p\text{Opt}}$ for maximizing η_{mp}^t in (25). However, the analytic solution for $\varphi_{p\text{Opt}}$ is very complex because parameters $k_{\varphi 1} \sim k_{\varphi 5}$ are determined by many unknown parameters including T_{hover} and Θ_m , which is impractical for the propeller design.

According to the Appendix, when the motor is not considered, there is an optimal pitch angle $\varphi_{p\text{Opt}0}$ for maximizing the propeller thrust efficiency η_p^t . However, when the motor and the propeller are considered as a whole, the pitch angle $\varphi_{p\text{Opt}0}$ will make the motor work under an inefficient state which decreases the total thrust efficiency η_{mp}^t . Therefore, the maximum motor-propeller efficiency solution $\varphi_{p\text{Opt}}$ from (25) should be smaller than the maximum propeller efficiency solution $\varphi_{p\text{Opt}0}$ from (39). As an example, a typical simulation result (motor: DJI 2312E KV960, $T_{\text{hover}} = 3.675$ N, $D_p = 10$ in, $H_p = 2.5 \sim 8$ in) to reveal the relationship between η_{mp}^t and φ_p is presented in Fig. 3, where $\varphi_{p\text{Opt}0} = 0.182$ is obtained from (39) in the Appendix and $\varphi_{p\text{Opt}} = 0.153$ is the solution for maximizing η_{mp}^t in (25).

In practice, a simplified estimation expression for $\varphi_{p\text{Opt}}$ is given by

$$\varphi_{p\text{Opt}} \approx k_c \cdot \varphi_{p\text{Opt}0} = k_c \sqrt[3]{\frac{3(\pi A + K_0)^2 C_{fd}}{\pi A K_0^2 \varepsilon^2}} \quad (26)$$

where $0 < k_c < 1$ is a correction coefficient. According to the simulation results, a good estimation effect can be obtained when $k_c \approx 0.85$. Noteworthy, the optimal pitch angle $\varphi_{p\text{Opt}}$ from (26) is only an estimated value, and a solution with higher precision can be obtained by solving (25).

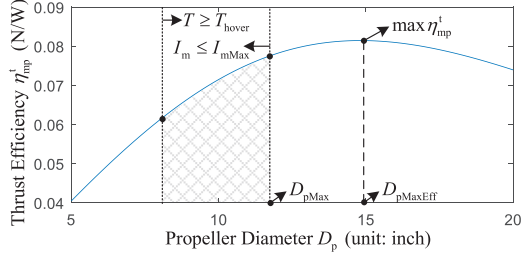


Fig. 4. Relationship between thrust efficiency and propeller diameter.

Remark 2: If the design task is to find an optimal propeller from a series of propeller products, and there are only a few propellers whose pitch angles φ_p are close to the optimal pitch angle φ_{pOpt} obtained from (26), then the optimal pitch angle φ_{pOpt} should be chosen according to the propeller product features. In this case, the optimal pitch angle φ_{pOpt} should be chosen as the mean value of the propeller candidates.

3) Optimal Diameter: According to (18), the thrust efficiency η_{mp}^t is written as

$$\eta_{mp}^t = \frac{1}{\frac{\pi^2 C_M^2 R_m T_{hover}}{900 K_E^2 C_T^2} D_p^2 + \frac{2\pi C_M T_{hover}^{0.5}}{\rho^{0.5} C_T^{1.5}} \frac{1}{D_p}}. \quad (27)$$

A simulation is performed for a propulsion system (motor: *JFRC-U3508*, propeller: $\varphi_p = 0.153$, $B_p = 2$, $T_{hover} = 10$ N) by fixing other parameters and changing the diameter D_p in (27), and the result is presented in Fig. 4. It is easy to observe from (27) that η_{mp}^t first increases then decreases as the propeller diameter D_p increases from 0 to ∞ . By applying the AM–GM inequality (36) in the Appendix to maximize η_{mp}^t in (27), it is easy to obtain the diameter $D_{pMaxEff}$ (unit: m) with the maximum thrust efficiency as

$$D_{pMaxEff} = \sqrt[3]{\frac{900 K_E^2}{\pi \rho C_M R_m} \sqrt{\frac{C_T}{\rho T_{hover}}}}. \quad (28)$$

However, the obtained diameter $D_{pMaxEff}$ is usually too large for the motor which may cause the exceeding of motor maximum current constraint in (19). Therefore, the optimal propeller diameter should be selected within the allowance range (mesh region in Fig. 4). The optimal propeller diameter should be determined by considering two situations

$$D_{pOpt} = \begin{cases} D_{pMax} & D_{pMaxEff} \geq D_{pMax} \\ D_{pMaxEff} & D_{pMaxEff} < D_{pMax} \end{cases}. \quad (29)$$

In practice, $D_{pMaxEff}$ is usually far larger than D_{pMax} as shown in Fig. 4. Therefore, the optimal propeller diameter D_{pOpt} is chosen as $D_{pOpt} = D_{pMax}$ in most cases.

C. Motor Optimization

Through the above propeller optimization procedures, the optimal propeller parameter set $\Theta_{pOpt} \triangleq \{D_{pOpt}, \varphi_{pOpt}, B_{pOpt}\}$ for a given motor Θ_m can be obtained. This section will introduce the method to choose the optimal motor–propeller combination for satisfying the given thrust requirements T_{hover} , T_{max} and maximizing the thrust efficiency η_{mp}^t . The algorithm is given as follows.

Algorithm 1: Searching Algorithm for the Optimal Motor.

Step 1: For each motor $\Theta_{m,i}$ in the motor database, find its optimal propeller parameters $\Theta_{pOpt,i}$ according to the propeller optimization method in Section III-B.

Step 2: Estimate the maximum thrust $T_{pMax,i}$ of each motor–propeller combination $\{\Theta_{m,i}, \Theta_{pOpt,i}\}$ through (21), and find the motor–propeller combinations with $T_{pMax,i}$ satisfying the maximum thrust constraint described by T_{max} in (7).

Step 3: Estimate the thrust efficiency $\eta_{mp,i}^t$ through (18) for the obtained motor–propeller combinations from Step 2, and find the optimal motor–propeller pair $\{\Theta_{mOpt}, \Theta_{pOpt}\}$ with the maximum thrust efficiency.

The algorithm complexity is proportional to the quantity of the motor products in the database, which is applicable in actual design procedures. It is easy to verify by using reduction to absurdity that the obtained result is the globally optimal solution under the given constraints. Note that the maximum thrust $T_{pMax,i}$ in Step 2 and η_{mp}^t in Step 3 can also be measured from the experimental data for higher precision.

D. Battery Optimization

After the propeller and motor are determined, the airframe can also be designed according to the principles in [3, pp. 57–71]. For simplicity, let $m_{other} \triangleq m_{copter} - m_{battery}$ represent the multicopter weight except for the battery. By combining (13), (14), (18), the battery discharge time as well as the multicopter hovering time t_{hover} is written as

$$\begin{aligned} t_{hover} &= \frac{60\eta_e\eta_b\rho_b \cdot m_{battery}}{m_{battery}g + m_{other}g} \cdot \eta_{mp}^t \\ &= \frac{60\eta_e\eta_b\rho_b \cdot m_{battery} \left(\frac{m_{battery}g + m_{other}g}{n_p}\right)^{-2}}{n_p R_m \left(\frac{\pi C_M D_p}{30 K_E C_T}\right)^2 + \frac{2\pi n_p C_M}{D_p \sqrt{\rho C_T^3}} \left(\frac{m_{battery}g + m_{other}g}{n_p}\right)^{-0.5}} \end{aligned} \quad (30)$$

where $m_{battery}$ should satisfy the constraint

$$T_{hover} = \frac{m_{battery}g + m_{other}g}{n_p} \leq \varepsilon_t T_{max} \quad (31)$$

where $\varepsilon_t \approx 0.9$ denotes a 10% thrust redundancy for the basic attitude control. The first row of (30) indicates that the hovering time t_{hover} of a multicopter is proportional to the thrust efficiency η_{mp}^t of the propulsion system, which proves the previous conclusion that increasing the thrust efficiency will lead to a longer time of endurance. It can also be concluded from (30) that the ESC efficiency η_e , the battery efficiency η_b , and the battery power density ρ_b should be chosen as large as possible to improve hovering time t_{hover} , which is consistent with practical experience.

A simulation is performed for a quadcopter (motor: *JFRC-U3508*, propeller: *APC 11 × 4.5*, battery: *LiPo-6S-22.2V*, other weight: $m_{other} = 3$ kg) by fixing other parameters and changing the battery weight $m_{battery}$ in (30), and the result is

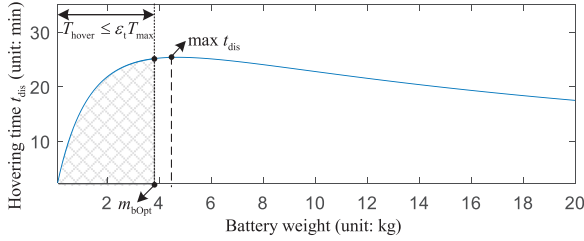


Fig. 5. Relationship between hovering time and battery weight.

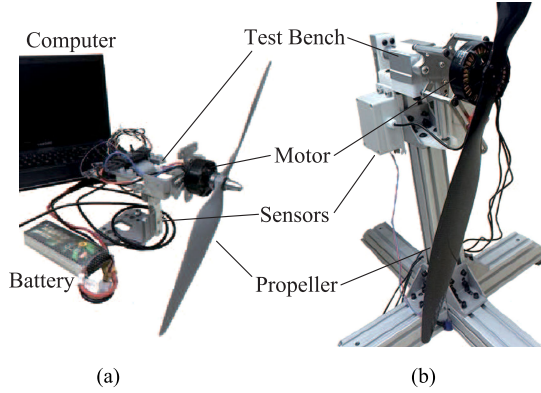


Fig. 6. Testing equipment for the propulsion system of multicopters.

presented in Fig. 5. It can be observed from Fig. 5 that the hovering time t_{hover} increases at first and then decreases as m_{battery} increases from 0 to ∞ . The decline of hovering time is caused by the decrease of thrust efficiency η_{mp}^t in (18) when the multicopter is too heavy. Noteworthy, limited by the thrust constraint in (31), the maximum value for t_{hover} in (30) is usually unreachable, and the optimal battery weight should be selected within the allowance range (mesh region in Fig. 5). In this case, the optimal battery weight m_{bOpt} is obtained on the boundary of the constraint in (31) as

$$m_{\text{bOpt}} = \frac{\varepsilon_t n_p T_{\text{max}} - m_{\text{other}} g}{g}.$$

Thus, according to (14), the optimal battery capacity C_{bOpt} is given by

$$C_{\text{bOpt}} = \frac{1000 \rho_b m_{\text{bOpt}}}{U_b}.$$

IV. EXPERIMENTS AND VERIFICATION

A. Experimental Equipment

For verifying the effectiveness of the proposed method, two test benches (see Fig. 6) are adopted to evaluate the performance of the multicopter propulsion system. These two test benches are both commercially available online with detailed descriptions on the product websites.^{1,2} The test benches can precisely

¹RCBenchmark. [Online]. Available: www.rcbenchmark.com/dynamometer-series-1580

²UAV Testbench V6. [Online]. Available: item.taobao.com/item.htm?id=546908746285

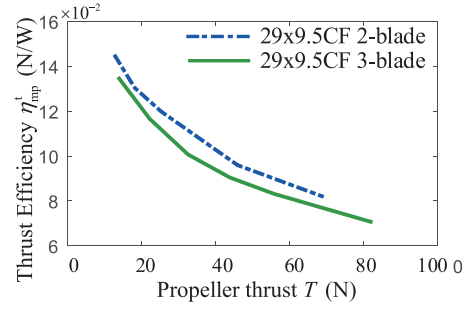


Fig. 7. Experimental results of three-blade and two-blade propellers.

TABLE II
HOVERING TESTS FOR A QUADCOPTER WITH WEIGHT:4 KG,
MOTOR:JFRC-U3508-KV550, BATTERY: 22.2 V-5500 MAH AND APC
PROPELLERS: 10–13 IN

| Propellers $D_p \times H_p$ (inches) | Motor full-throttle current (A) | Battery current (A) | Thrust efficiency (N/W) | Hovering time (min) |
|--|---------------------------------------|---------------------------|-------------------------------|---------------------------|
| $\leq 11 \times 3$ | ≤ 10 | ≥ 32 | ≤ 0.055 | ≤ 9.4 |
| 11x4.5 | 13.1 | 26 | 0.068 | 11.5 |
| 11x5.5 | 15.5 | 24.9 | 0.071 | 12.1 |
| 12x4.5 | 19 | 22.6 | 0.078 | 13.3 |
| $\geq 12 \times 5.5$ | > 20 | - | - | - |

measure the input power and the output thrust of a propulsion system, which is convenient to analyze the thrust efficiency of a propulsion system, and estimate the hovering time of a multicopter.

B. Optimization Method Verification

With the test benches in Fig. 6, a series of tests are performed to verify the optimization method proposed in Section III.

1) **Blade Number Tests:** A series of experiments are performed to verify the relationship between the thrust efficiency and the blade number. The selected propellers are the T-MOTOR 29×9.5 CF series propellers (diameter: 29 in, pitch: 9.5 in) with two blades and three blades (other parameters are the same), and the experimental results are shown in Fig. 7. It can be concluded from the results in Fig. 7 that two-blade propellers have higher thrust efficiency for generating the same thrust. The experimental results agree with the theoretical analysis in (23), which also explains why most propellers available on the market are two-blade propellers.

2) **Pitch and Diameter Tests:** Table II presents the hovering test results of a multicopter assembling different propellers, where the propellers are from the APC website³ with the diameter D_p varying from 10 to 13 in and the pitch H_p varying from 3 to 5.5 in. The measured parameters of the tested motor JFRC-U3508 are given by

$$K_V = 550 \text{ r/min/V}, U_{m\text{Max}} = 22.2 \text{ V}, I_{m\text{Max}} = 20 \text{ A}, \\ U_{m0} = 10 \text{ V}, I_{m0} = 0.5 \text{ A}, R_m = 0.3 \Omega, U_b = 22.2 \text{ V} \quad (32)$$

³[Online]. Available: <https://www.apcprop.com/>

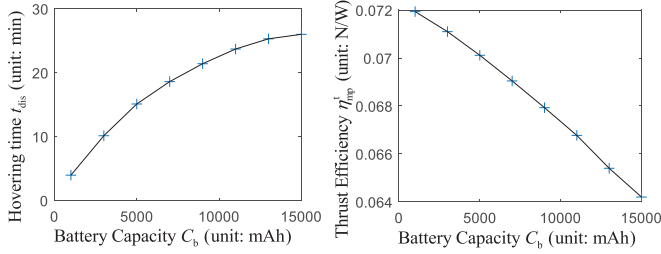


Fig. 8. Hovering tests for a quadcopter with different battery capacity.

and the blade parameters in (10) are calibrated according to experimental data in [15] and given by

$$\begin{aligned} A &= 5, \varepsilon = 0.85, \lambda = 0.7, \zeta = 0.5 \\ e &= 1, C_{fd} = 0.01, K_0 = 6.11, \alpha_t = 0.89. \end{aligned} \quad (33)$$

By substituting the parameters (32), (33) into (25), (27), (30), the simulation results for the motor *JFRC-U3508* have already been presented in Figs. 3–5 in Section III. As a result, the optimal pitch angle is obtained from (26) as $\varphi_{pOpt} \approx 0.153$ rad, the maximum diameter is obtained from (22) as $D_{pMax} \approx 11.7$ in, and the maximum efficiency diameter is obtained from (28) as $D_{pMaxEff} \approx 15$ in. Therefore, the theoretically optimal propeller parameters for motor *JFRC-U3508* are obtained from (24), (26), (29) as $B_{pOpt} = 2$, $D_{pOpt} = 11.7$ in, $H_{pOpt} = \pi D_{pOpt} \tan(\varphi_{pOpt}) = 5.58$ in.

It can be observed from Table II that the hovering time (thrust efficiency) of a multicopter can be significantly improved by optimizing the propeller selection for the motor. The thrust efficiency η_{mp}^t in Table II increases as the pitch angle φ_p and the diameter D_p increase, which is consistent with the theoretical expectations because the propellers are in the increasing range ($D_p \leq D_{pMaxEff}$ and $\varphi_p \leq \varphi_{pOpt}$) of (25), (27). Table II also shows that the motor may be overheated (full-throttle current exceeds the upper limit $I_{mMax} = 20$ A) when the propeller is too large ($\geq 12 \times 5.5$), which is consistent with the result $D_{pMax} \approx 11.7$ in estimated by the proposed method. Since the parameters of propeller products are usually discrete as presented in Table II, the obtained optimal propeller parameters B_{pOpt} , D_{pOpt} , H_{pOpt} may not exactly point to an available propeller product, but it provides a result close enough to the optimal solution. In this case, the optimal propeller in Table II is APC 12×4.5 , which is the one with parameters closed to theoretical solution B_{pOpt} , D_{pOpt} , H_{pOpt} from the proposed method.

3) Battery Tests: A series of hovering tests are performed for a popular *F450* quadcopter (motor and propeller: T-MOTOR MN2212 KV920 + 9.5×4.5). By changing the battery capacity from 1000 to 15000 mAh (the total weight of the quadcopter changes from 1.1 to 2.22 kg), the results of the hovering time and thrust efficiency are presented in Fig. 8. The results in Fig. 8 shows that the hovering time t_{hover} increases as the battery capacity C_b increases, which is consistent with the theoretical simulation analysis in Fig. 5. Since the maximum capacity obtained from the weight constraint in

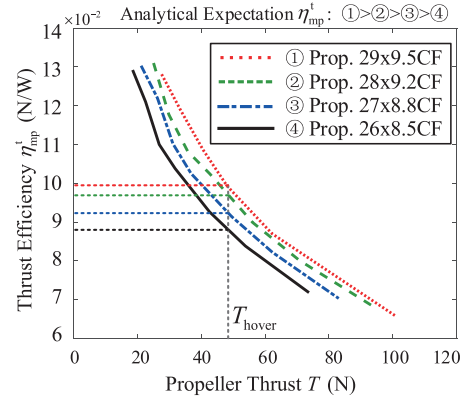


Fig. 9. Motor thrust efficiency test for propellers with different diameters.

(31) is $C_{bMax} = 15300$ mAh, the optimal battery capacity is obtained as $C_{bOpt} = C_{bMax} = 15300$ mAh, which is close to the experimental results in Fig. 8. However, although the quadcopter has the maximum hovering time in this case, the control performance of the quadcopter is very bad in flight tests because the total weight is too heavy ($T_{hover}/T_{max} > 0.9$) for the current propulsion system. Besides, it can be observed in Fig. 8 that the growth of the hovering time becomes very slow when C_b increases from 10000 to 15000 mAh, which is because the thrust efficiency decreases rapidly in this range. If more factors (hovering time, control performance, payload capacity) is considered, 8000 mAh may be a better choice for the practical usage. In summary, the proposed method is effective to find the battery with the maximum hovering time, but the selection of battery capacity should consider more factors in practice.

C. Propeller Selection Case

In this part, the motor U11 KV90 is adopted as an example to find its optimal propeller diameter through experimental analysis. The optimal blade number is chosen as $B_{pOpt} = 2$ and the optimal pitch angle is chosen as $\varphi_{pOpt} = 0.107$ rad according to the statistical analysis in Remark 2 for available propeller products on the website [24]. The optimal propeller diameter obtained from (29) is $D_{pOpt} = D_{pMax} \approx 29$ in, which is consistent with the recommendation result based on the experimental test data in [24].

In order to verify that the motor–propeller system has the maximum thrust efficiency when $D_{pOpt} = 29$ in in practice, thrust efficiency tests are performed for U11 KV90 with diameters changing from 26 to 29 in, and the test results are shown in Fig. 9. It can be observed from Fig. 9 that the thrust efficiency η_{mp}^t increases as the propeller diameter D_p increases and the output thrust T_{hover} decreases, which coincides with the relationship in (27). Results in Fig. 9 show that the obtained optimal diameter $D_{pOpt} = 29$ in has the maximum thrust efficiency. Thus, the proposed optimization method gives the same result as the experimental method that the optimal propeller for U11 KV90 should be 29×9.5 CF.

TABLE III
PART OF THE OPTIMAL MOTOR SELECTION ALGORITHM RESULTS

| Motor model | Motor weight | Voltage U_{mMax} | Propeller Θ_{pOpt} | Thrust T_{pMax} | η_{mp}^t at $T=49N$ |
|---------------|--------------|--------------------|---------------------------|-------------------|--------------------------|
| U10II KV100 | 0.415 kg | 48 V | 29x9.5 | 93.7 N | - |
| U10Plus KV100 | 0.514 kg | 48 V | 26x8.5 3-Blade | 97.6 N | 0.085 N/W |
| U11 KV90 | 0.792 kg | 48 V | 29x9.5 | 98.8 N | 0.094 N/W |
| U12 KV100 | 0.715 kg | 50 V | 30x10.5 | 130.0 N | - |
| U13 KV85 | 1.3 kg | 48 V | 30x10.5 | 158.5 N | - |

D. Multicopter Design Case

Assuming that the design task is to find the optimal propulsion system for a quadcopter ($m_{copter} = 20$ kg, $n_p = 4$, $a_c = 9.8$ m/s², $\rho = 1.2$ kg/m³), the propulsion system design requirements from (1)–(3) are obtained as $T_{hover} = 49$ N and $T_{max} = 98$ N. Then, the optimization algorithm in Section III-C is applied for motor and propeller products from [24], and some typical results near the optimal solution are listed in Table III. The optimal combination obtained from Table III is motor U11 KV90 + propeller 29×9.5 CF, which has the maximum thrust $T_{pMax} = 98.8$ N closest to the desired value 98 N and the highest thrust efficiency $\eta_{mp}^t = 0.094$ N/W under the hovering thrust T_{hover} . After the motor and propeller are both determined, the ESC and the battery can also be determined according to the hovering time curve in Fig. 5 and the actual control performance. Therefore, the proposed method is capable of quickly determining the optimal propulsion system with the given design requirements.

E. Comparison With Other Methods

Since the total computation amount is proportional to the motor product number n_m in the database, the selection program is fast enough [algorithm complexity $O(n_m)$] to be finished within 30 ms by using a web server with low configuration. Considering that the existing numerical methods [11]–[14] consume minutes or even hours [algorithm complexity $O(n_m^4)$] to traverse all the possible component combinations, the proposed method is faster and more efficient.

V. CONCLUSION

This paper proposed a practical method to help designers quickly determine the optimal propulsion system to maximize the efficiency of the propulsion system under the desired flight condition. The parameters that may affect the hovering time of multicopters are studied respectively based on the theoretical analysis, which may help designers to optimize the parameters for a more efficient multicopter design. In most cases, the thrust efficiency of the propulsion system will first increase then decrease as a parameter (diameter, pitch angle, battery capacity) increases to infinity. However, limited by constraints, the maximum points are usually unreachable and the optimal solution occurs on the boundary of the constraints. Since the method is based on theoretical calculation, the precision of the obtained result depends on the precision of the component parameters, so experimental measurement or system identification are

recommended in the actual application of the method. Experiments, simulations, and design cases demonstrate the effectiveness and practicability of the proposed method. During the battery design, it is interesting to find that the control ability may be significantly reduced when increasing the battery capacity for the maximum hovering time. Therefore, multicopter design optimization method with comprehensively considering more factors will be studied in the future. Along with the aerodynamic modeling for the body and the wing, the proposed method will also be extended to optimize the efficiency of fixed-wing aircraft or vertical takeoff and landing aircraft. The safety and reliability of multicopter UAVs are also very important in the future. Therefore, further study is required for selecting components according to their reliability characteristics to make sure the obtained UAV satisfy the safety requirements.

APPENDIX

A. Propeller Thrust Efficiency Optimization

If only the propeller is considered, the propeller thrust efficiency η_p^t (unit: N/W) is defined as

$$\eta_p^t = \frac{T_{hover}}{P_{pHover}} = \frac{T_{hover}}{M_{hover} \cdot \frac{2\pi}{60} N_{hover}}. \quad (34)$$

Substituting (10), (15) into (34) gives

$$\eta_p^t = \frac{D_p}{2\pi} \frac{\sqrt{\rho}}{\sqrt{T_{hover}}} \frac{\sqrt{C_T}}{C_M} = \frac{k_{p0}}{\varphi_p^{0.5} + \frac{(\pi A + K_0)^2 \epsilon C_{fd}}{\pi A K_0^2 \epsilon^2} \varphi_p^{-1.5}} \quad (35)$$

where k_{p0} is a positive value irrelevant to φ_p . It is easy to observe from (35) that the propeller thrust efficiency η_p^t first increases then decreases as φ_p increases from 0 to ∞ . The arithmetic and geometric (AM-GM) inequality is introduced here

$$(x_1 + x_2 + \dots + x_n) / n \geq \sqrt[n]{x_1 \cdot x_2 \cdot \dots \cdot x_n} \quad (36)$$

and that equality holds if and only if $x_1 = x_2 = \dots = x_n$. Then, by applying the AM-GM inequality (36) to (35), one has

$$\begin{aligned} \eta_p^t &= \frac{k_{p0}}{\frac{1}{3}\varphi_p^{0.5} + \frac{1}{3}\varphi_p^{0.5} + \frac{1}{3}\varphi_p^{0.5} + \frac{(\pi A + K_0)^2 \epsilon C_{fd}}{\pi A K_0^2 \epsilon^2} \varphi_p^{-1.5}} \\ &\leq \frac{k_{p0}}{4 \cdot \sqrt[4]{\left(\frac{1}{3}\varphi_p^{0.5}\right)^3 \cdot \frac{(\pi A + K_0)^2 \epsilon C_{fd}}{\pi A K_0^2 \epsilon^2} \varphi_p^{-1.5}}} \end{aligned} \quad (37)$$

and η_p^t in (37) takes the maximum value when

$$\frac{1}{3}\varphi_p^{0.5} = \frac{(\pi A + K_0)^2 \epsilon C_{fd}}{\pi A K_0^2 \epsilon^2} \varphi_p^{-1.5}. \quad (38)$$

Thus, it is easy to obtain the propeller optimal pitch angle φ_{pOpt0} in (39) by solving (38) as

$$\varphi_{pOpt0} = \sqrt{\frac{3(\pi A + K_0)^2 C_{fd}}{\pi A K_0^2 \epsilon^2}}. \quad (39)$$

REFERENCES

- [1] C. Luo, L. Yu, and P. Ren, "A vision-aided approach to perching a bioinspired unmanned aerial vehicle," *IEEE Trans. Ind. Electron.*, vol. 65, no. 5, pp. 3976–3984, May 2018, doi: [10.1109/TIE.2017.2764849](https://doi.org/10.1109/TIE.2017.2764849).
- [2] Q. Fu, Q. Quan, and K. Y. Cai, "Robust pose estimation for multirotor UAVs using off-board monocular vision," *IEEE Trans. Ind. Electron.*, vol. 64, no. 10, pp. 7942–7951, Oct. 2017, doi: [10.1109/TIE.2017.2696482](https://doi.org/10.1109/TIE.2017.2696482).
- [3] Q. Quan, *Introduction to Multicopter Design and Control*. Singapore: Springer, 2017.
- [4] D. Lawrence and K. Mohseni, "Efficiency analysis for long duration electric MAVs," in *Proc. Infotech@Aerosp. Conf.*, Sep. 2005, doi: [10.2514/6.2005-7090](https://doi.org/10.2514/6.2005-7090).
- [5] M. Ahtelik, K.-M. Doth, D. Gurdan, and J. Stumpf, "Design of a multi rotor MAV with regard to efficiency, dynamics and redundancy," in *Proc. AIAA Guid., Navigat., Control Conf.*, Aug. 2012, doi: [10.2514/6.2012-4779](https://doi.org/10.2514/6.2012-4779).
- [6] A. Cavagnino, G. Bramerdorfer, and J. A. Tapia, "Optimization of electric machine designs—Part I," *IEEE Trans. Ind. Electron.*, vol. 64, no. 12, pp. 9716–9720, Dec. 2017, doi: [10.1109/TIE.2017.2753359](https://doi.org/10.1109/TIE.2017.2753359).
- [7] G. Allaka, B. Anasuya, C. Yamini, N. Vaidehi, and Y. V. Ramana, "Modelling and analysis of multicopter frame and propeller," *Int. J. Res. Eng. Technol.*, vol. 2, no. 4, pp. 481–483, 2013.
- [8] D. Gamble and A. Arena, "Automated dynamic propeller testing at low Reynolds numbers," in *Proc. 48th AIAA Aerosp. Sci. Meeting Including New Horizons Forum Aerosp. Expo.*, Jan. 2010, doi: [10.2514/6.2010-853](https://doi.org/10.2514/6.2010-853).
- [9] H.-I. Kwon, S. Yi, and S. Choi, "Design of efficient propellers using variable-fidelity aerodynamic analysis and multilevel optimization," *J. Propulsion Power*, vol. 31, no. 4, pp. 1057–1072, 2015, doi: [10.2514/1.B35097](https://doi.org/10.2514/1.B35097).
- [10] D. Lundström and P. Krus, "Micro aerial vehicle design optimization using mixed discrete and continuous variables," in *Proc. 11th AIAA/ISSMO Multidisciplinary Anal. Optim. Conf.*, Sep. 2006, doi: [10.2514/6.2006-7020](https://doi.org/10.2514/6.2006-7020).
- [11] D. Lundstrom, K. Amadori, and P. Krus, "Distributed framework for micro aerial vehicle design automation," in *Proc. 46th AIAA Aerosp. Sci. Meeting Exhib.*, Jan. 2008, doi: [10.2514/6.2008-140](https://doi.org/10.2514/6.2008-140).
- [12] D. Lundström, K. Amadori, and P. Krus, "Automation of design and prototyping of micro aerial vehicle," in *Proc. 47th AIAA Aerosp. Sci. Meeting Including New Horizons Forum Aerosp. Expo.*, Jan. 2009, doi: [10.2514/6.2009-629](https://doi.org/10.2514/6.2009-629).
- [13] Ø. Magnussen, G. Hovland, and M. Ottestad, "Multicopter UAV design optimization," in *Proc. IEEE/ASME 10th Int. Conf. Mechatronic Embedded Syst. Appl.*, Sep. 2014, pp. 1–6, doi: [10.1109/MESA.2014.6935598](https://doi.org/10.1109/MESA.2014.6935598).
- [14] Ø. Magnussen, M. Ottestad, and G. Hovland, "Multicopter design optimization and validation," *Modeling, Identification Control*, vol. 36, no. 2, pp. 67–79, 2015, doi: [10.4173/mic.2015.2.1](https://doi.org/10.4173/mic.2015.2.1).
- [15] D. Shi, X. Dai, X. Zhang, and Q. Quan, "A practical performance evaluation method for electric multicopters," *IEEE/ASME Trans. Mechatronics*, vol. 22, no. 3, pp. 1337–1348, 2017, doi: [10.1109/TMECH.2017.2675913](https://doi.org/10.1109/TMECH.2017.2675913).
- [16] M. Cavcar, "The international standard atmosphere (ISA)," Anadolu Univ., Eskişehir, Turkey, vol. 30, p. 9, 2000.
- [17] D. Bershadsky, S. Haviland, and E. N. Johnson, "Electric multirotor UAV propulsion system sizing for performance prediction and design optimization," in *Proc. 57th AIAA/ASCE/AHS/ASC Structures, Structural Dyn., Mater. Conf.*, Jan. 2015, doi: [10.2514/6.2016-0581](https://doi.org/10.2514/6.2016-0581).
- [18] M. Merchant and L. S. Miller, "Propeller performance measurement for low Reynolds number UAV applications," in *Proc. 44th AIAA Aerosp. Sci. Meeting Exhib.*, Jan. 2006, doi: [10.2514/6.2006-1127](https://doi.org/10.2514/6.2006-1127).
- [19] R. S. Merrill, "Nonlinear aerodynamic corrections to blade element momentum modul with validation experiments," Utah State Univ., Logan, UT, USA, Tech. Rep. Paper 67, 2011.
- [20] R. E. Sheldahl and P. C. Klimas, "Aerodynamic characteristics of seven symmetrical airfoil sections through 180-degree angle of attack for use in aerodynamic analysis of vertical axis wind turbines," Sandia Nat. Labs, Albuquerque, NM, USA, Tech. Rep. SAND-80-2114, 1981.
- [21] R. Deters, "Performance and slipstream characteristics of small-scale propellers at low Reynolds numbers," Ph.D. dissertation, Aerospace Engineering in the Graduate College, University of Illinois at Urbana-Champaign, 2014.
- [22] M. S. Selig and G. Ananda, "Low Reynolds number propeller performance data: Wind tunnel corrections for motor fixture drag," *Aerosp. Eng.*, no. 1, pp. 1–4, 2011.
- [23] S. Chapman, *Electric Machinery Fundamentals*. Ahmedabad, Gujarat: Tata McGraw-Hill Education, 2005.
- [24] M. Wu, "T-motor official website," Accessed on: Sep. 28, 2018. [Online]. Available: <http://store-en.tmotor.com/>



Xunhua Dai received the B.S. and M.S. degrees in control science and engineering from Beihang University, Beijing, China, in 2013 and 2016, respectively. He is currently working toward the Ph.D. degree with the School of Automation Science and Electrical Engineering, Beihang University, Beijing, China.

His main research interests include reliable flight control, learning control, model-based design, and optimization of UAVs.



Quan Quan received the B.S. and Ph.D. degrees in control science and engineering from Beihang University, Beijing, China, in 2004 and 2010, respectively.

He has been an Associate Professor with Beihang University since 2013, where he is currently with the School of Automation Science and Electrical Engineering. His research interests include reliable flight control, vision-based navigation, repetitive learning control, and time-delay systems.



Jinrui Ren received the B.S. degree in control science and engineering from Northwestern Polytechnical University, Xi'an, China, in 2014. She is currently working toward the Ph.D. degree with the School of Automation Science and Electrical Engineering, Beihang University, Beijing, China.

Her main research interests include nonlinear control, flight control, and aerial refueling.



Kai-Yuan Cai received the B.S., M.S., and Ph.D. degrees in control science and engineering from Beihang University, Beijing, China, in 1984, 1987, and 1991, respectively.

He has been a Full Professor at Beihang University since 1995. He is a Cheung Kong Scholar (Chair Professor), jointly appointed by the Ministry of Education of China and the Li Ka Shing Foundation of Hong Kong in 1999. His main research interests include software testing, software reliability, reliable flight control, and

software cybernetics.